

Research



Cite this article: Kimoto M, Tan HP, Tan YS, Mislan NABM, Hirao I. 2023 Success probability of high-affinity DNA aptamer generation by genetic alphabet expansion. *Phil. Trans. R. Soc. B* **378**: 20220031.
<https://doi.org/10.1098/rstb.2022.0031>

Received: 27 April 2022

Accepted: 18 June 2022

One contribution of 15 to a theme issue 'Reactivity and mechanism in chemical and synthetic biology'.

Subject Areas:

biotechnology, biomaterials

Keywords:

SELEX, DNA library, DNA aptamer, unnatural bases, genetic alphabet expansion

Authors for correspondence:

Michiko Kimoto

e-mail: michiko.kimoto@xenolis.com

Ichiro Hirao

e-mail: ichiro.hirao@xenolis.com

Electronic supplementary material is available online at <https://doi.org/10.6084/m9.figshare.c.6328848>.

Success probability of high-affinity
DNA aptamer generation by genetic
alphabet expansion

Michiko Kimoto^{1,2}, Hui Pen Tan^{1,2}, Yaw Sing Tan^{1,3},
Nur Afiqah Binte Mohd Mislan^{1,2} and Ichiro Hirao^{1,2}

¹Xenolis Pte Ltd, 79 Science Park Drive, #06-01/08, Cintech IV, Singapore 118264, Singapore

²Institute of Bioengineering and Bioimaging, Agency for Science, Technology and Research (A*STAR), 31 Biopolis Way, #07-01 Nanos, Singapore 138669, Singapore

³Bioinformatics Institute, A*STAR, 30 Biopolis Street, #07-01 Matrix, Singapore 138671, Singapore

MK, 0000-0002-6261-7562; YST, 0000-0002-2522-9421; IH, 0000-0002-1115-8079

Nucleic acid aptamers as antibody alternatives bind specifically to target molecules. These aptamers are generated by isolating candidates from libraries with random sequence fragments, through an evolutionary engineering system. We recently reported a high-affinity DNA aptamer generation method that introduces unnatural bases (UBs) as a fifth letter into the library, by genetic alphabet expansion. By incorporating hydrophobic UBs, the affinities of DNA aptamers to target proteins are increased over 100-fold, as compared with those of conventional aptamers with only the natural four letters. However, there is still plenty of room for improvement of the methods for routinely generating high-affinity UB-containing DNA (UB-DNA) aptamers. The success probabilities of the high-affinity aptamer generation depend on the existence of the aptamer candidate sequences in the initial library. We estimated the success probabilities by analysing several UB-DNA aptamers that we generated, as examples. In addition, we investigated the possible improvement of conventional aptamer affinities by introducing one UB at specific positions. Our data revealed that UB-DNA aptamers adopt specific tertiary structures, in which many bases including UBs interact with target proteins for high affinity, suggesting the importance of the UB-DNA library design.

This article is part of the theme issue 'Reactivity and mechanism in chemical and synthetic biology'.

1. Introduction

Nucleic acid aptamers are single-stranded DNA or RNA molecules that bind specifically to a wide variety of targets, such as small molecules, sugars, proteins and cells. Aptamers are generated by an evolutionary engineering method called SELEX (systematic evolution of ligands by exponential enrichment), through repetitive processes of selection and amplification using nucleic acid libraries with randomized sequences [1,2]. Once the aptamer sequences have been determined by SELEX, the aptamers and their modifications are manufactured by solid-phase chemical synthesis and can be used as antibody alternatives. However, one main issue is the aptamers' insufficient affinities to targets, because of the limited chemical diversity, especially the low hydrophobicity, of the nucleic acid components, A, G, C and T/U, for interactions with hydrophobic regions of target proteins. Thus, the practical applications of nucleic acid aptamers are still limited, and many improved methods for modified aptamer generation have been reported [3–8]. Especially, the use of a chemically expanded library is widely considered to be advantageous for generating high-affinity aptamers, but few studies have experimentally or theoretically confirmed the validity of this strategy [9].

Recently, we developed a novel DNA aptamer generation method called ExSELEX (genetic alphabet Expansion for SELEX), in which a hydrophobic unnatural base (UB), 7-(2-thienyl)-imidazo [4,5-*b*] pyridine (Ds), is introduced as a fifth letter [10–13] (electronic supplementary material, figure S1). The Ds-containing DNA (Ds-DNA) fragments can be amplified by polymerase chain reaction (PCR) using the unnatural base pair (UBP) between Ds and 2-nitro-4-propynylpyrrole (Px) [14,15] (figure 1*a*), allowing Ds-DNA aptamer generation by ExSELEX. We generated several high-affinity Ds-DNA aptamers with 0.65–132 pM K_D values, targeting vascular endothelial growth factor 165 (VEGF₁₆₅), interferon γ (IFN γ) [10], von Willebrand factor A1-domain (vWF) [16] and each serotype of dengue NS1 proteins [17] (figure 1*b*). However, the generation of Ds-DNA aptamers with high affinities (sub-nanomolar K_D) is still a laborious and intricate process with low success probabilities, because of the higher complexity when the fifth letter is included than in the four-letter DNA aptamer generation.

In the SELEX process, the complexity (number of different sequences) in the library is a key to increasing the success probability of high-affinity aptamer generation, which relies on the existence of aptamer candidates in the initial library [7,9,18–23]. Greater complexity in the initial library increases the success probability of aptamer generation. However, a typical SELEX procedure limits the complexities to 10^{12} – 10^{15} different sequences, owing to the scale of the handling volume and the concentration of DNA/RNA. For example, a representative modified RNA aptamer ($K_D = 10$ pM), an initial precursor (v.30.44) of pegaptanib [24], targeting VEGF₁₆₅ was obtained from 1 nmol of a modified RNA library with a 30-base random region (N30), which contains 6.02×10^{14} sequences ($10^{-9} \times$ Avogadro's constant) [25] (electronic supplementary material, figure S2). The aptamer consists of 19 internal stem-loop bases and a 4-bp terminal stem. If each of the 19 bases in the internal stem-loop regions is essential or important and any base pairs are acceptable in the 4-bp terminal stem, then the occurrence of the 27-mer aptamer candidates would be $(6.02 \times 10^{14} \times 12)/(7.0 \times 10^{13} = 4^{(19+4)})$ in the library containing N30 and primer regions, suggesting that approximately 103 aptamer candidate sequences were included in 1 nmol of the initial N30 library (refer to electronic supplementary material, figure S2 for the calculation).

In ExSELEX with the fifth letter, the complexity of the library becomes greater and more intricate than that of the conventional four-letter libraries, theoretically reducing the success probability of high-affinity aptamer generation owing to the scale limitations of the initial library. In general, the possible number of all the different sequences in the N30 library with the four natural letters is $4^{30} \approx 1.15 \times 10^{18}$. However, the number in the N30 library with the randomized five letters increases to $5^{30} \approx 9.31 \times 10^{20}$, indicating that only 10^{14} – 10^{15} different sequences (0.0001–0.001% of the total complexity) in the number are used in ExSELEX.

Here, we analysed the ExSELEX data for the high-affinity aptamers that we generated, to estimate the success probabilities of Ds-DNA aptamer generation from the viewpoint of five-letter DNA libraries. For the analysis, we determined the essential or important bases in the four Ds-DNA aptamers targeting IFN γ , vWF and dengue virus serotypes 1 and 3 NS1 proteins by a gel electrophoresis mobility shift assay (EMSA). We also examined the Ds incorporation into a conventional four-letter DNA aptamer, ARC1172, targeting vWF, to determine whether the hydrophobic UB improves the

aptamer affinity, and rationalized the data by structural modelling. These results reveal the importance of both the specific bases including Ds and the unique tertiary structures of each aptamer, providing information for further improvements in the design of UB-DNA libraries.

2. Material and methods

(a) Materials

DNA aptamer variants, listed in electronic supplementary material, tables S1–S5, were chemically synthesized with an Oligonucleotide synthesizer nS-8 (Gene Design) or an H8 DNA/RNA Synthesizer (K&A Laborgerate), using phosphoramidite reagents for the natural and Ds bases. The Ds phosphoramidite was prepared as described previously [26], and the phosphoramidites for the natural bases were purchased from Glen Research. The synthesized DNA fragments were purified by denaturing gel electrophoresis before use. Recombinant proteins, human vWF A1-domain (vWF: amino acids 1238–1481), human IFN γ , and dengue virus serotype-1 NS1 (DEN1-NS1) and serotype-3 NS1 (DEN3-NS1), were purchased from U-Protein Express, Peprotech and Native Antigen Company, respectively.

(b) Electrophoresis mobility shift assay

The relative binding efficiency of each aptamer variant to the target protein was determined by EMSA, as described previously [16,17,27]. The conditions for the binding and gel electrophoresis, along with their respective buffers, are summarized in electronic supplementary material, table S6. The relative binding efficiency of each aptamer variant with the target protein was determined from the shifted band patterns on the gels, detected with a LAS-4000 bioimager (Fuji Film) after staining with SYBR Gold. The band densities of free and complexed DNAs were quantified using the Multigauge software (Fuji Film), and the relative binding (%) was calculated by normalization with the shifted ratio for the original aptamer in the same gel.

(c) Molecular dynamics simulations

To investigate the target interactions with some of the substituted variants of ARC1172, we performed molecular dynamics (MD) simulations. Details of the preparation of the starting structures, MD simulations and binding free energy calculations are described in the electronic supplementary material.

3. Results

(a) Success probability of high-affinity aptamer generation by ExSELEX

First, we reviewed the success probability of the high-affinity Ds-DNA aptamer ($K_D < \text{nM}$) generation by considering seven aptamers that we generated by ExSELEX, targeting VEGF₁₆₅, IFN γ , vWF and four dengue virus serotypes of NS1 proteins (DEN1-NS1 to DEN4-NS1) (figure 1*b*). These aptamers were isolated from single-stranded Ds-DNA libraries with 10^{14} – 10^{15} different sequences (complexities) (figure 1*c*), after 7–10 rounds of selection and PCR amplification. All of the isolated aptamer candidates with high affinities had specific sequences containing two or three Ds bases, flanked by complementary terminal stem regions (figure 1*b*).

In the anti-VEGF₁₆₅, IFN γ , DEN1-NS1, DEN2-NS1, DEN3-NS1 and DEN4-NS1 aptamer generations, we used a mixture of Ds-predetermined sublibraries (DP library) (electronic

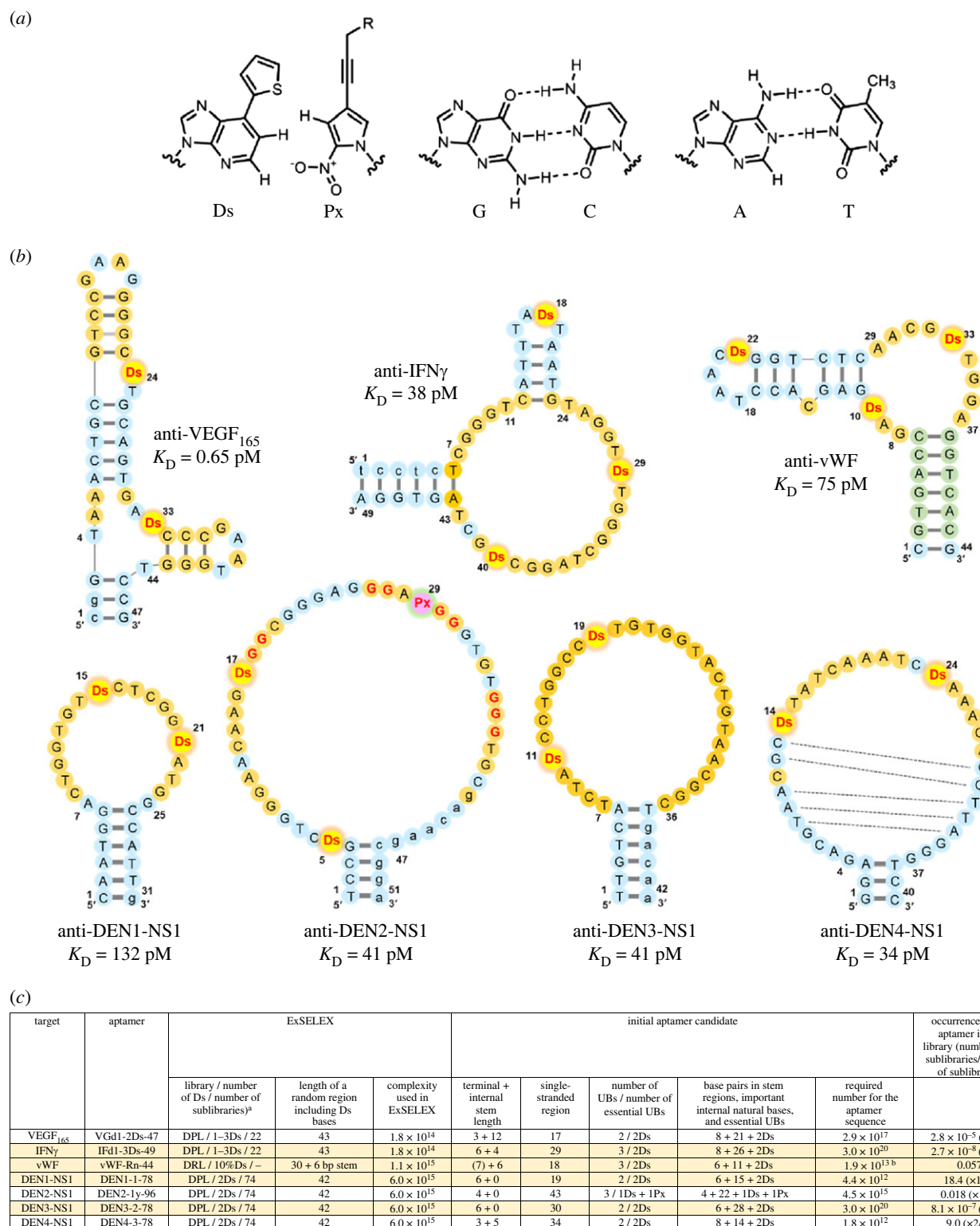


Figure 1. High-affinity Ds-DNA aptamer candidates obtained by ExSELEX. (a) Chemical structures of a hydrophobic unnatural base pair, Ds–Px, and the natural A–T and G–C base pairs. (b) Predicted secondary structures of high-affinity Ds-DNA aptamers targeting VEGF₁₆₅, IFN γ , von Willebrand factor A1-domain (vWF), and each serotype of dengue NS1 proteins. For the anti-DEN1/2/3/4-NS1 aptamers, their core parts are shown by removing the flanking primer regions. The bases in the randomized and primer regions are shown in large and small letters, respectively. The important bases (orange circles) were estimated from the doped selections (anti-VEGF₁₆₅ and anti-IFN γ aptamers) or the obtained sequence motifs (anti-DEN1-, DEN2- and DEN4-NS1 aptamers). There is no information available for anti-vWF and DEN3-NS1, and thus the loop regions are tentatively estimated as the important bases. Green circles in the anti-vWF aptamer are the original constant complementary sequences for stem formation. In the anti-DEN2-NS1 aptamer, the four G tracts that form a G-quadruplex structure are shown by red Gs. The dashed lines in the anti-DEN4-NS1 aptamer represent a stem region found in the internal loop region. (c) Estimation of the occurrence of the aptamer candidates in the initial library based on ExSELEX data. (Online version in colour.)

supplementary material, figure S1c), in which one to three Ds bases are embedded at specific positions within a natural base randomized region. For the anti-VEGF₁₆₅ and IFN γ

aptamer generation, 22 sublibraries (total complexity: 1.8×10^{14}) with one to three Ds bases were used [10], and for each serotype of anti-DEN-NS1 aptamer generation, 74 sublibraries

(total complexity: 6×10^{15}) with two Ds bases were used [17]. In the anti-vWF aptamer generation, we employed a Ds-randomized (five-letter-randomized) library (DR library; complexity: 1.1×10^{15}) consisting of 10% Ds and 22.5% each natural base in an N30 region flanked by conserved complementary 6-base sequences that form a stem, as well as PCR primer sequences [16] (electronic supplementary material, figure S1e).

The isolated anti-IFN γ and vWF aptamers contain three Ds bases. After the characterization and optimization of each aptamer, we determined that two Ds bases, at positions 29 and 40 in the anti-IFN γ aptamer and positions 10 and 33 in the anti-vWF aptamer, are essential for their high affinities (figure 1b). The non-essential Ds bases at position 18 for anti-IFN γ and position 22 for anti-vWF are each located in a small loop region, which can be replaced with a more stable mini-hairpin sequence (electronic supplementary material, figure S3) [16,28,29].

The anti-DEN2-NS1 aptamer contains one Px base at position 29, as well as two Ds bases. The Px base is the pairing partner of Ds for PCR amplification, and this Px base in the aptamer appeared by the misincorporation of Px opposite natural bases in templates during PCR in ExSELEX. This Px at position 29 and one Ds at position 17 are essential for high-affinity binding, and the other Ds at position 5 is not essential. The anti-DEN2-NS1 aptamer forms a G-quadruplex structure with four G tracts shown by red Gs in figure 1b [17].

The success probability of each aptamer generation was estimated from the occurrence of the aptamer in the library, which was determined from the complexity in the initial library divided by the required number for the aptamer candidate sequence in each ExSELEX (figure 1c). The required number for the aptamer candidate sequence, in which at least one aptamer sequence possibly appears, was determined using the number of essential/important bases and the stem length in each aptamer. The important bases are indicated in orange-coloured circles in the secondary structures in figure 1b. Each important base was estimated by the data obtained from the second ExSELEX, using doped libraries for anti-VEGF₁₆₅ and IFN γ aptamer generation, in which we chose greater than 96% conservation of bases [10], or from the conserved sequences in the isolated clones for anti-DEN-NS1 aptamer generation [17]. For example, in the anti-VEGF₁₆₅ aptamer, there are 21 important natural bases including two stem regions, as well as 2 Ds bases, and 8 bp, in which any base pairs are acceptable, in the terminal and internal stem regions. Thus, the required number for the aptamer sequences is $4^{(21+8)} = 2.9 \times 10^{17}$. In the anti-DEN3-NS1 aptamer generation, only one sequence in the isolated clones was obtained, and no consensus sequences in the clone were identified. Thus, in the calculation of the anti-DEN3-NS1 aptamer, we used all of the bases (28 natural bases and 2 Ds bases) in the loop region and the 6-bp terminal stem, and the tentative required number for the aptamer sequence is $4^{(28+6)} = 3.0 \times 10^{20}$. From the sequencing data of the anti-DEN4-NS1 aptamer generation, we found stem regions in the internal loop region (figure 1b), and thus the aptamer contains 8 bp (three in terminal and five in loop regions) in the secondary structure.

In the anti-vWF aptamer generation using the DR library, we determined the required number for the aptamer sequence by a different method. The regions of the terminal stem and the loop at positions 18–22 were ignored in the calculation, because the terminal stem was embedded into the

initial library as a constant sequence, and the bases in the loop regions were not essential for tight binding. Since we had no data about the important bases in the other regions, all 13 bases (including two Ds bases) in the single-stranded region were treated as the important bases in the five letters, and two internal stem regions were treated as the stems with non-essential bases. Thus, the required number for the anti-vWF aptamer is $5^{(13+6)} = 1.9 \times 10^{13}$.

From these required numbers for each aptamer sequence and the complexities of each initial library used, we calculated the occurrence of the aptamer in the library, which is the theoretical number of aptamer candidate sequences found in the initial libraries (figure 1c). In ExSELEX using DP libraries, the complexity of the initial library was divided by the required numbers for the sequence and by the total sublibrary number used, and then multiplied by the number of the sublibraries that include two Ds bases at the same interval (-Ds-N_r-Ds-) and appropriate positions ('number of hit sublibraries' in figure 1c). For example, the occurrence of the aptamer in the library for the anti-DEN4-NS1 aptamer generation is $((6.0 \times 10^{15}) / (1.8 \times 10^{13})) \times 2 / 74 \approx 9.0$, since two of the 74 sublibraries have two Ds bases at the same interval and appropriate positions compared with the aptamer. As for the anti-DEN2-NS1 aptamer, only one Ds base is essential, and thus the aptamer could possibly be isolated from all 74 sublibraries. In the anti-vWF aptamer generation, we calculated the occurrence of the aptamer in the library by a different method owing to the use of the DR library (refer to figure 1c and electronic supplementary material, figure S4).

The occurrence of the aptamer candidates in the library (figure 1c) revealed that the library size used for most of the aptamer generations, except for the anti-DEN1-NS1, DEN2-NS1 and DEN4-NS1 aptamers, was too small. However, the aptamers were successfully obtained from the libraries, suggesting that some factors used for the calculation might not reflect that fact. One of the uncertainties in the calculation is the determination of the important or essential bases in each aptamer. Thus, we re-evaluated the important/essential bases in the single-stranded regions of some aptamers, focusing on the anti-IFN γ , vWF, DEN1-NS1 and DEN3-NS1 aptamers, by EMSA using a series of sequence variants for each aptamer.

For the assay, we chemically synthesized a variant set for each aptamer by point transition mutation ($A \leftrightarrow G$, $T \leftrightarrow C$) in the single-stranded regions. We used the optimized sequences for some aptamers, as shown in electronic supplementary material, figure S3 and tables S1–S4. In the optimization, the terminal stem lengths were extended and the A–T pairs were replaced with G–C pairs in the stem of each aptamer [10,12,17,29]. The small internal stem–loop sequences in the anti-IFN γ and vWF aptamers were replaced with thermally stable mini-hairpin sequences, CGCGAAGCG or CCGAAGG [16,29] (electronic supplementary material, tables S1 and S2). Therefore, these two aptamers are highly stabilized thermally. Binding analyses of these anti-IFN γ and anti-vWF aptamers to their targets were performed using 25 nM aptamer variants and 50 nM target proteins, and the complexes were separated from the free DNA by electrophoresis on a gel containing 3 M urea at 30–37°C for EMSA. In our ExSELEX procedure, we had employed stringent washing conditions of the DNA–target complexes to isolate high-affinity aptamers. As a result, some aptamers had very high affinities (less than several tens of pM K_D values) to their targets. Thus, we used the gel

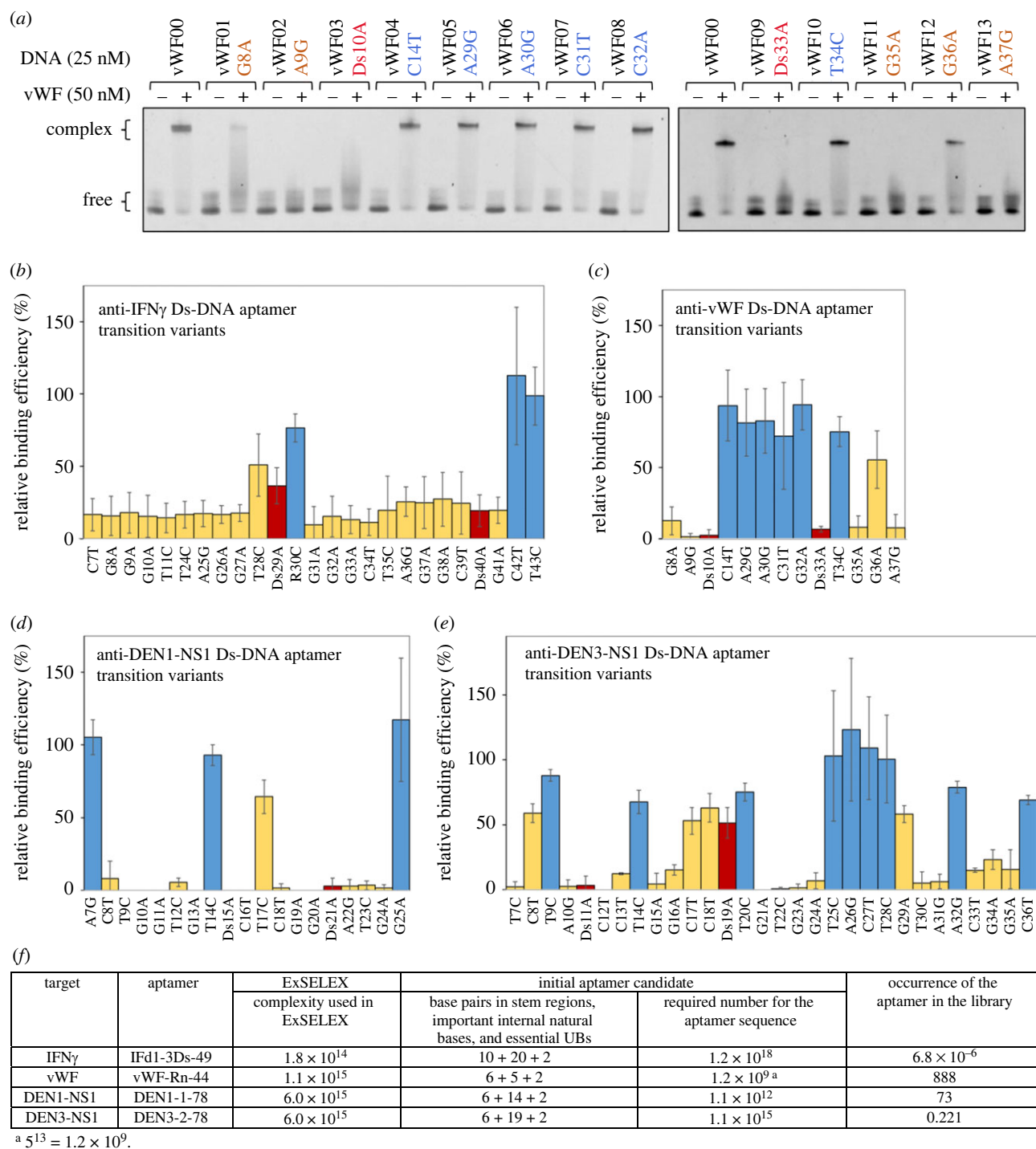


Figure 2. Binding analysis of Ds-DNA aptamer variants with point transition mutations. (a) EMSA for the anti-vWF Ds-DNA aptamer variants. (b–e) Relative binding efficiencies (%) of each variant of anti-IFN γ Ds-DNA aptamer (b), anti-vWF Ds-DNA aptamer (c), anti-DEN1-NS1 Ds-DNA aptamer (d), and anti-DEN3-NS1 Ds-DNA aptamer (e), determined with normalization of the complex formation efficiency of each original Ds-DNA aptamer (electronic supplementary material, figure S3) from EMSA (electronic supplementary material, figures S5–S7). The Ds positions are shown by red bars. The positions that exhibited less than 65% of the relative binding efficiencies (average) were assigned as the essential base positions and are shown by orange bars. (f) Re-estimation of the occurrence of the aptamer candidates in the initial library used, according to the important/essential bases identified by EMSA. (Online version in colour.)

analysis conditions in the presence of 3 M urea for anti-IFN γ and anti-vWF aptamers and their variants to identify the differences between their nanomolar and picomolar K_D values [16] (figure 2a; electronic supplementary material, figure S5 and table S6). The binding analyses of anti-DEN1-NS1 and anti-DEN3-NS1 aptamers, which have no internal mini-hairpin sequences, were performed using 50 nM aptamer variants and 25 nM of each DEN-NS1 hexamer, and the complexes were detected on a native gel at 30°C, in the absence of urea (electronic supplementary material, figures S6 and S7 and

table S6). The anti-DEN1-NS1 aptamer has an additional mini-hairpin sequence, CGCGAAGCG, at its 3'-terminus [17] (electronic supplementary material, table S3), since its target binding was slightly lower than that of the anti-DEN3-NS1 aptamer and the terminal stem stability affected its affinity (data not shown).

The binding proportion (%) of the complex of each aptamer and its variants with target proteins was measured from the band densities of the complex and the unbound aptamer. The relative binding efficiencies of each aptamer variant

relative to the original aptamer are summarized in figure 2*b–e*. The binding efficiencies of most of the variants for each aptamer were lower than those of the original one, and some base mutations significantly reduced the binding to their targets. Each mutated base position that exhibited less than 65% of the relative binding efficiencies (average) was assigned as an important base position for high-affinity binding (sub-nanomolar K_D) in each aptamer, based on our previous EMSA results [27].

We re-calculated the required numbers for aptamer sequences and the occurrence of the aptamer in the library for the anti-IFN γ , vWF, DEN1-NS1 and DEN3-NS1 aptamers, using the important bases determined by the EMSA experiments (figure 2*f*). Since the numbers of essential or important bases obtained by EMSA are smaller than those in figure 1*c*, reasonable numbers of the anti-vWF, DEN1-NS1 and DEN3-NS1 aptamer sequences are included in the initial library. However, the occurrence of the anti-IFN γ aptamer in the library is still very low, and, theoretically, a library with 1.2×10^{18} complexity would be required for this aptamer generation.

(b) High-affinity aptamer generation by natural to unnatural base mutations in conventional aptamers

Another intriguing issue of UB-DNA aptamer generation is whether high-affinity Ds-DNA aptamers can be obtained by replacing any natural base with Ds in known four-letter aptamers. As a model system, we chose the 41-mer DNA aptamer targeting vWF, ARC1172 (or ARC1779), which inhibits vWF binding to platelet-receptor glycoprotein Iba and is under phase II clinical trials [30–33]. Based on the secondary structure of the aptamer and the tertiary structure in the complex with vWF [34] (figure 3*a*), we chemically synthesized two sets of its variants; variants with a point transition mutation and variants with the Ds replacement of each base in the single-stranded regions (positions 7, 8, 10, 21, 22, 27–31) (electronic supplementary material, table S5). The relative binding efficiencies (%) of each variant in the two sets were determined by EMSA, using 100 nM of each aptamer variant and 200 nM vWF (figure 3*b*; electronic supplementary material, figure S8 and table S6). The data revealed that the positions at T10 and G28 were acceptable as the Ds replacement positions, while the original natural bases at positions 8, 10, 21, 22 and 27 are relatively important for the tight binding. However, the affinities of two variants, T10Ds and G28Ds, did not exceed that of the original aptamer.

To assess the potential binding sites for Ds, we first performed ligand-mapping molecular dynamics (LMMD) simulations to identify potential Ds replacement positions in ARC1172. LMMD is a computational pocket detection method that uses small organic molecules called fragments to rapidly identify binding pockets in MD simulations [35–38]. Since the Ds nucleotide is highly hydrophobic, benzene was used as the probe of choice in the simulations.

Based on the benzene occupancy maps generated from LMMD simulations of vWF, we identified three hydrophobic binding sites near the aptamer binding interface. These hydrophobic binding sites are close to the sites where T10, G28 and T31 of ARC1172 bind (figure 3*c*), and positions T10 and G28 are consistent with the data from the Ds replacement experiments. The results support that the Ds base interacts with a hydrophobic region in vWF. The T10 site

corresponds to the binding site of Leu110 in botrocetin, a snake venom protein that binds to vWF and promotes dysfunctional platelet aggregation (electronic supplementary material, figure S9*a*), while the T31 site corresponds to the binding site of Tyr291 in botrocetin and Tyr316 of the anti-vWF antibody NMC-4 (electronic supplementary material, figure S9*b,c*). The significant decline in the relative binding efficiency of the T31Ds variant might be attributed to steric clashes introduced by the bulkier nitrogenous base of Ds (figure 3*d*), while C31, being a pyrimidine base like thymine, is still acceptable for the binding, as shown in figure 3*b*.

To understand the tolerance at positions T10 and G28 for the Ds replacement, we next performed MD simulations of vWF complexed with T10Ds and G28Ds variants. Since the T10 and G28 bases are solvent-exposed, the perturbation of the tertiary structures by the Ds replacement is likely to be minor. As expected, both variants remained bound to vWF throughout the simulations, with little deviation from the initial conformation. The calculated binding free energies of the Ds-replaced variants are not significantly different from that of ARC1172 (electronic supplementary material, table S7). The 1-deazapurine and thiophene moieties of T10Ds alternated between two flipped conformations during the simulations, suggesting that the thiophene ring neither interacts strongly nor enhances vWF binding significantly (figure 3*e*). As a comparison, the hydrophobic interaction of the thiophene ring of the G28Ds variant only partially compensated for the loss of hydrogen bonding between G28 and Glu1389 in the original aptamer, hence resulting in its moderate affinity (figure 3*f*).

For further understanding, we also analysed one of the low-affinity variants, T27C, by MD simulations. In ARC1172, T27 forms hydrogen bonds with the amide oxygen and backbone nitrogen of Gln1391, which allows the adjacent G26 to move closer to vWF and interact with the backbone nitrogen of Arg1392 (electronic supplementary material, figure S10*a*). These hydrogen bonds are maintained in the MD simulations (electronic supplementary material, figure S10*b*). However, thymine has reversed positions of hydrogen bond-donating and -accepting atoms from cytosine. This leads to electrostatic repulsion between C27 and Gln1391. MD simulations of the T27C variant complexed with vWF show that the DNA segment from G26 to C27 cannot approach as close to vWF as that of ARC1172. C27 moves away from vWF and instead only forms hydrogen bonds with the amide side chain of Gln1391. This results in a loss of hydrogen bonding interactions between G26 and vWF (electronic supplementary material, figure S10*c*). The computed average binding free energy of the T27C variant is less negative than that of ARC1172 (electronic supplementary material, table S7), which agrees with the EMSA experiments. The surface plasmon resonance (SPR) analysis of the original aptamer and T27C variant also showed that the transition mutation T27C reduced the affinity to vWF (electronic supplementary material, figure S10*d*).

We also checked the root mean square deviation (RMSD) for each MD result, focusing on the C α backbone of vWF in ligand mapping, as well as the C α and DNA backbone atoms in the complexes of vWF with ARC1172, the T10Ds variant, the G28Ds variant and the T27C variant (electronic supplementary material, figures S11 and S12). The plot patterns confirmed that each MD simulation reached a good steady state.

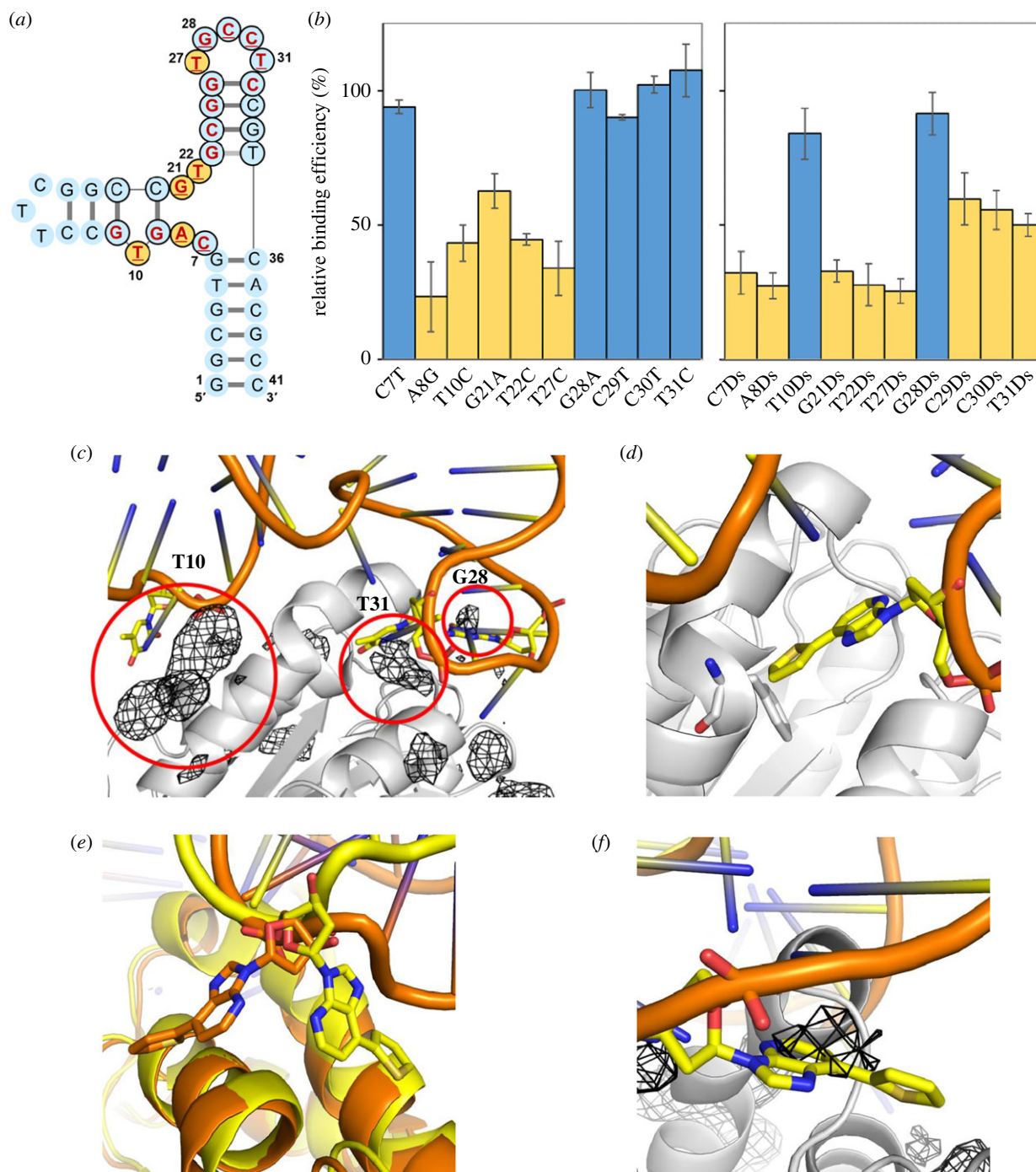


Figure 3. Binding of ARC1172 variants with vWF. (a) Schematic illustration of ARC1172. Nucleotides with bold red letters are within 4.2 Å of vWF in the complex [34]. The consensus nucleotides identified for high-affinity binding to vWF are indicated in black circles [34]. The 10 positions for point mutations (transition or Ds incorporation) are underlined. The essential bases assigned from the EMSA (electronic supplementary material, figure S8) are shown in orange circles. (b) Relative binding efficiencies (%) of ARC1172 variants with vWF. The positions that exhibited less than 65% of the relative binding efficiencies (average) were assigned as the essential base positions and are shown by orange bars. (c) Binding sites detected near the aptamer–vWF binding interface. Benzene occupancy maps (black mesh) overlaid on the structure of ARC1172 complexed with vWF (PDB 3HXQ), with detected binding sites near the aptamer–vWF binding interface circled in red. vWF is shown in white, and the aptamer is shown in yellow and orange. (d) Modelled structure of the vWF–ARC1172 (T31Ds) complex, showing steric clash between Ds31 (yellow) and Phe1397 (white). (e) MD snapshots of the vWF–ARC1172 (T10Ds) complex, showing alternative conformations of Ds10 (yellow and orange). (f) MD snapshot of the vWF–ARC1172 (G28Ds) complex, showing the overlap of Ds28 with the benzene map densities (black mesh). (Online version in colour.)

4. Discussion

The research of UB-DNA aptamer generation methods has just barely started, and only two types of UBPs, Ds–Px and Z–P, have been used [10,13,39–41]. The additional letters significantly increase the chemical diversity of libraries, augmenting the aptamers' affinities but reducing the success

probabilities of UB-DNA aptamer generation. Here, from the viewpoint of the library size and complexity, we estimated the success probabilities of the Ds-DNA aptamers that we have generated so far. The results, obtained by considering the important or essential bases and stem structures in each aptamer, revealed that the isolated aptamer sequences targeting vWF and the series of DEN-NS1 proteins possibly existed

in their initial libraries, and so these high-affinity aptamers were generated with high success rates. The anti-DEN2-NS1 aptamer contains one Px base, which was accidentally misincorporated by mutation during the ExSELEX procedure, and thus it was a serendipitous result. In addition, a mutation occurring during the PCR amplification step plays an important role to increase the sequence diversity of a library with limited complexity [10,39].

Our results for the anti-IFN γ and anti-VEGF₁₆₅ aptamers indicated the difficulty of generating these aptamers, and that a library with greater complexity (approx. 10^{18}) might be required. These two aptamer generations were our first success. It must have been beginners' luck because we later improved the DP library for the anti-DEN-NS1 aptamer generation, increasing the occurrence of each anti-DEN-NS1 aptamer generation in the library, which contains only two essential Ds bases at every position in the natural base randomized region. From this aspect, we should more rationally investigate why these anti-IFN γ and anti-VEGF₁₆₅ aptamers were generated against incredible odds. Most of the Ds-DNA aptamers contain two essential Ds bases, which are sufficient to exhibit high affinities to their targets (sub-nanomolar K_D values). These two Ds bases in the five aptamers are separated by 5–10 natural bases. Some, but not all, of the natural bases are important for the tight binding. Our LMMD simulations demonstrated that the highly hydrophobic Ds base interacts with a hydrophobic site in target proteins. Since the Ds bases significantly contribute to the tight binding to targets, one plausible speculation is that, first, two Ds bases interact with two hydrophobic sites on the target protein, and then surrounding natural base sequences interact or fit with the target surface areas. In this stage, several different natural base sequence contexts might be available for the tight binding. In the RNA aptamer generation targeting MS2 coat proteins, a different sequence from the native MS2 RNA that binds to its coat proteins was isolated, and the X-ray crystallography of the complex revealed that the binding features of the RNA aptamer were very similar to those of the native MS2 RNA even with the different sequence context and the secondary structures [42]. Therefore, several sequence variations of the natural bases between or around the two Ds bases could be employed for high-affinity binding, and we successfully isolated one such sequence in the anti-IFN γ and anti-VEGF₁₆₅ aptamer generation, even from the DP library with limited complexity.

The two Ds and specific natural bases might form a unique tertiary structure to fit the shape of each target protein. The terminal stem that always appears in the high-affinity Ds-DNA aptamers could stabilize the tertiary structure. Our Ds replacement experiments for ARC1172 did not show any further improvement of the aptamer affinity by only a replacement of the natural base with Ds at the appropriate positions, indicating the importance of suitable natural base sequence contexts around the Ds bases, which were obtained from the library by ExSELEX. The combination of two Ds and some natural bases in a specific structure is important for high-affinity UB-DNA aptamer generation, and thus the significant improvement of natural base-DNA aptamers that have already been generated, only by replacing some natural bases with Ds, can be difficult, as shown in the anti-vWF Ds-DNA aptamer generation.

We have two types of libraries, DP and DR, and most of the high-affinity UB-DNA aptamers were obtained by ExSELEX using the DP libraries. Our representative aptamer generated

by using the DR library is the anti-vWF aptamer. Since two Ds bases are sufficient for high-affinity DNA aptamer generation, DP libraries with two Ds bases are more suitable than DR libraries. In our 42-mer DP library containing two Ds bases for anti-DEN-NS1 aptamer generation, the total possible number with different sequence contexts is $4^{40} \approx 1.2 \times 10^{24}$ in each sublibrary. By contrast, the number in a 42-mer DR library is increased to $5^{42} \approx 2.3 \times 10^{29}$, reducing the success probability of aptamer generation. Furthermore, in the N30 library with 10% Ds bases used for the anti-vWF aptamer generation, only 22.8% of the sequences contained two Ds bases (electronic supplementary material, figure S4), and the other sequences containing more than four or five Ds bases reduced the PCR amplification efficiencies in ExSELEX. Even so, the anti-vWF aptamer generation succeeded, because only six natural bases in the single-stranded region of the aptamer were important for the tight binding, and 888 aptamer candidate sequences existed in the initial DR library (figure 2f). On the other hand, one of the strong points of the DR library is that the terminal stem sequences can be embedded within the library, as shown in the N30 DR library for anti-vWF aptamer generation [16] (electronic supplementary material, figure S1e). To incorporate the terminal stem sequence into the DP library, we must prepare many sublibraries for all combinations of two Ds base contexts in the single-stranded region of the library.

As one of the limitations of this study using the doped libraries and the transition mutation variants, note that our current estimation to identify the important bases supposes a simplified situation, including a degree of uncertainty. For example, in anti-IFN γ and anti-VEGF₁₆₅ aptamer generation, we used the results obtained by a second ExSELEX with the doped library to determine the essential bases and stem regions in the aptamer. However, such a library does not include hit sequences with random insertions or deletions. The doped selection of the anti-VEGF₁₆₅ aptamer revealed that the two loop sequences, GAAG (positions 16–19) and GAAT (positions 37–40), contain two important bases (underlined and in bold), but another analysis using non-essential nucleotide-deletion variants (position 19 or/and 40) showed the loss of the binding affinity [28]. Although this might be a special case, in which a stable mini-hairpin sequence appeared by this deletion, causing loss of the affinity, this shows that not all deletions of non-essential bases are acceptable. In our analysis using mutation variants, we employed only transition mutations to simplify the method and did not strictly examine all of the variants with other mutations, including transversions. In addition, we assumed that any stem sequences are acceptable, but some stem sequences complementary to a loop region could cause substantial changes in the proper aptamer folding and affect the affinity to targets.

This study illustrates some potentially useful considerations during aptamer generation or optimization. The design of DP and DR libraries for ExSELEX might be further improved. Using the results of LMMD simulation of potential UB (Ds) binding sites of a target protein (vWF), more appropriate DP sublibrary sets can be chosen, without expending excessive resources. During optimization of a high-affinity DNA aptamer, the method of screening its transition mutation variants using EMSA offers a simple method to identify the important bases as an initial screening.

Data accessibility. The data are provided in electronic supplementary material [43].

Authors' contributions. M.K.: conceptualization, data curation, formal analysis, investigation, methodology, supervision, validation, writing—original draft, writing—review and editing; H.P.T.: data curation, methodology, validation, writing—review and editing; Y.S.T.: conceptualization, data curation, formal analysis, investigation, methodology, software, validation, writing—original draft, writing—review and editing; N.A.B.M.M.: data curation, investigation, writing—review and editing; I.H.: conceptualization, data curation, investigation, methodology, supervision, validation, writing—original draft, writing—review and editing.

All authors gave final approval for publication and agreed to be held accountable for the work performed herein.

Conflict of interest declaration. We have no competing interests.

Funding. This work was supported by the Institute of Bioengineering and Bioimaging and the Bioinformatics Institute (Biomedical Research Council, Agency for Science, Technology and Research, Singapore) and the 2021 Horizontal Technology Programme Office Seed Fund at A*STAR grant no. (C-21-13-18-002).

Acknowledgements. We thank Ms Yurina Saiki for assistance with some of the EMSA experiments for ARC 1172.

References

1. Tuerk C, Gold L. 1990 Systematic evolution of ligands by exponential enrichment: RNA ligands to bacteriophage T4 DNA polymerase. *Science* **249**, 505–510. (doi:10.1126/science.2200121)
2. Ellington AD, Szostak JW. 1990 *In vitro* selection of RNA molecules that bind specific ligands. *Nature* **346**, 818–822. (doi:10.1038/346818a0)
3. Röhrlisberger P, Hollenstein M. 2018 Aptamer chemistry. *Adv. Drug. Deliv. Rev.* **134**, 3–21. (doi:10.1016/j.addr.2018.04.007)
4. Zhou J, Rossi J. 2017 Aptamers as targeted therapeutics: current potential and challenges. *Nat. Rev. Drug Discov.* **16**, 440. (doi:10.1038/nrd.2017.86)
5. Meek KN, Rangel AE, Heemstra JM. 2016 Enhancing aptamer function and stability via *in vitro* selection using modified nucleic acids. *Methods* **106**, 29–36. (doi:10.1016/j.ymeth.2016.03.008)
6. Gawande BN, Rohloff JC, Carter JD, von Carlowitz I, Zhang C, Schneider DJ, Janjic N. 2017 Selection of DNA aptamers with two modified bases. *Proc. Natl Acad. Sci. USA* **114**, 2898–2903. (doi:10.1073/pnas.1615475114)
7. Pfeiffer F, Rosenthal M, Siegl J, Ewers J, Mayer G. 2017 Customised nucleic acid libraries for enhanced aptamer selection and performance. *Curr. Opin. Biotechnol.* **48**, 111–118. (doi:10.1016/j.copbio.2017.03.026)
8. McKenzie LK, El-Khoury R, Thorpe JD, Damha MJ, Hollenstein M. 2021 Recent progress in non-native nucleic acid modifications. *Chem. Soc. Rev.* **50**, 5126–5164. (doi:10.1039/d0cs01430c)
9. Gold L *et al.* 2010 Aptamer-based multiplexed proteomic technology for biomarker discovery. *PLoS ONE* **5**, e15004. (doi:10.1371/journal.pone.0015004)
10. Kimoto M, Yamashige R, Matsunaga K, Yokoyama S, Hirao I. 2013 Generation of high-affinity DNA aptamers using an expanded genetic alphabet. *Nat. Biotechnol.* **31**, 453–457. (doi:10.1038/Nbt.2556)
11. Kimoto M, Matsunaga K, Hirao I. 2016 DNA aptamer generation by genetic alphabet expansion SELEX (ExSELEX) using an unnatural base pair system. *Methods Mol. Biol.* **1380**, 47–60. (doi:10.1007/978-1-4939-3197-2_4)
12. Hirao I, Kimoto M, Lee KH. 2017 DNA aptamer generation by ExSELEX using genetic alphabet expansion with a mini-hairpin DNA stabilization method. *Biochimie* **145**, 15–21. (doi:10.1016/j.biochi.2017.09.007)
13. Kimoto M, Hirao I. 2020 Genetic alphabet expansion technology by creating unnatural base pairs. *Chem. Soc. Rev.* **49**, 7602–7626. (doi:10.1039/d0cs00457j)
14. Kimoto M, Kawai R, Mitsui T, Yokoyama S, Hirao I. 2009 An unnatural base pair system for efficient PCR amplification and functionalization of DNA molecules. *Nucleic Acids Res.* **37**, e14. (doi:10.1093/nar/gkn956)
15. Yamashige R, Kimoto M, Takezawa Y, Sato A, Mitsui T, Yokoyama S, Hirao I. 2012 Highly specific unnatural base pair systems as a third base pair for PCR amplification. *Nucleic Acids Res.* **40**, 2793–2806. (doi:10.1093/nar/gkr1068)
16. Matsunaga K, Kimoto M, Hirao I. 2017 High-affinity DNA aptamer generation targeting von Willebrand factor A1-domain by genetic alphabet expansion for systematic evolution of ligands by exponential enrichment using two types of libraries composed of five different bases. *J. Am. Chem. Soc.* **139**, 324–334. (doi:10.1021/jacs.6b10767)
17. Matsunaga K, Kimoto M, Lim VW, Tan HP, Wong YQ, Sun W, Vasoo S, Leo YS, Hirao I. 2021 High-affinity five/six-letter DNA aptamers with superior specificity enabling the detection of dengue NS1 protein variants beyond the serotype identification. *Nucleic Acids Res.* **49**, 11407–11424. (doi:10.1093/nar/gkab515)
18. Charlton J, Smith D. 1999 Estimation of SELEX pool size by measurement of DNA renaturation rates. *RNA* **5**, 1326–1332. (doi:10.1017/s1355838299991021)
19. Sharma TK, Bruno JG, Dhiman A. 2017 ABCs of DNA aptamer and related assay development. *Biotechnol. Adv.* **35**, 275–301. (doi:10.1016/j.biotechadv.2017.01.003)
20. Kohlberger M, Gadermaier G. 2021 SELEX: critical factors and optimization strategies for successful aptamer selection. *Biotechnol. Appl. Biochem.* **69**, 1771–1792. (doi:10.1002/bab.2244)
21. Qian S, Chang D, He S, Li Y. 2022 Aptamers from random sequence space: accomplishments, gaps and future considerations. *Anal. Chim. Acta* **1196**, 339511. (doi:10.1016/j.aca.2022.339511)
22. Wang T, Chen C, Larcher LM, Barrero RA, Veedu RN. 2019 Three decades of nucleic acid aptamer technologies: lessons learned, progress and opportunities on aptamer development. *Biotechnol. Adv.* **37**, 28–50. (doi:10.1016/j.biotechadv.2018.11.001)
23. Vorobyeva MA, Davydova AS, Vorobjev PE, Venyaminova AG. 2018 Key aspects of nucleic acid library design for *in vitro* selection. *Int. J. Mol. Sci.* **19**, 470. (doi:10.3390/ijms19020470)
24. Ng EW, Shima DT, Calias P, Cunningham ET Jr, Guyer DR, Adamis AP. 2006 Pegaptanib, a targeted anti-VEGF aptamer for ocular vascular disease. *Nat. Rev. Drug Discov.* **5**, 123–132. (doi:10.1038/nrd1955)
25. Ruckman J, Green LS, Beeson J, Waugh S, Gillette WL, Henninger DD, Claesson-Welsh L, Janjic N. 1998 2'-Fluoropyrimidine RNA-based aptamers to the 165-amino acid form of vascular endothelial growth factor (VEGF165). Inhibition of receptor binding and VEGF-induced vascular permeability through interactions requiring the exon 7-encoded domain. *J. Biol. Chem.* **273**, 20556–20567. (doi:10.1074/jbc.273.32.20556)
26. Hirao I, Kimoto M, Mitsui T, Fujiwara T, Kawai R, Sato A, Harada Y, Yokoyama S. 2006 An unnatural hydrophobic base pair system: site-specific incorporation of nucleotide analogs into DNA and RNA. *Nat. Methods* **3**, 729–735. (doi:10.1038/nmeth915)
27. Kimoto M, Sherman Lim YW, Hirao I. 2019 Molecular affinity rulers: systematic evaluation of DNA aptamers for their applicabilities in ELISA. *Nucleic Acids Res.* **47**, 8362–8374. (doi:10.1093/nar/gkz688)
28. Kimoto M, Nakamura M, Hirao I. 2016 Post-ExSELEX stabilization of an unnatural-base DNA aptamer targeting VEGF165 toward pharmaceutical applications. *Nucleic Acids Res.* **44**, 7487–7494. (doi:10.1093/nar/gkw619)
29. Matsunaga K, Kimoto M, Hanson C, Sanford M, Young HA, Hirao I. 2015 Architecture of high-affinity unnatural-base DNA aptamers toward pharmaceutical applications. *Scient. Rep.* **5**, 18478. (doi:10.1038/srep18478)
30. Oney S, Nimjee SM, Layzer J, Que-Gewirth N, Ginsburg D, Becker RC, Arepally G, Sullenger BA. 2007 Antidote-controlled platelet inhibition targeting von Willebrand factor with aptamers. *Oligonucleotides* **17**, 265–274. (doi:10.1089/oli.2007.0089)
31. Gilbert JC *et al.* 2007 First-in-human evaluation of anti von Willebrand factor therapeutic aptamer ARC1779 in healthy volunteers. *Circulation* **116**, 2678–2686. (doi:10.1161/CIRCULATIONAHA.107.724864)

32. Diener JL, Daniel Lagasse HA, Duerschmied D, Merhi Y, Tanguay JF, Hutabarat R, Gilbert J, Wagner DD, Schaub R. 2009 Inhibition of von Willebrand factor-mediated platelet activation and thrombosis by the anti-von Willebrand factor A1-domain aptamer ARC1779. *J. Thromb. Haemost.* **7**, 1155–1162. (doi:10.1111/j.1538-7836.2009.03459.x)
33. Mayr FB, Knobl P, Jilma B, Siller-Matula JM, Wagner PG, Schaub RG, Gilbert JC, Jilma-Stohlawetz P. 2010 The aptamer ARC1779 blocks von Willebrand factor-dependent platelet function in patients with thrombotic thrombocytopenic purpura ex vivo. *Transfusion* **50**, 1079–1087. (doi:10.1111/j.1537-2995.2009.02554.x)
34. Huang RH, Fremont DH, Diener JL, Schaub RG, Sadler JE. 2009 A structural explanation for the antithrombotic activity of ARC1172, a DNA aptamer that binds von Willebrand factor domain A1. *Structure* **17**, 1476–1484. (doi:10.1016/j.str.2009.09.011)
35. Tan YS, Sledz P, Lang S, Stubbs CJ, Spring DR, Abell C, Best RB. 2012 Using ligand-mapping simulations to design a ligand selectively targeting a cryptic surface pocket of polo-like kinase 1. *Angew. Chem. Int. Edn Engl.* **51**, 10078–10081. (doi:10.1002/anie.201205676)
36. Tan YS, Spring DR, Abell C, Verma C. 2014 The use of chlorobenzene as a probe molecule in molecular dynamics simulations. *J. Chem. Inf. Model.* **54**, 1821–1827. (doi:10.1021/ci500215x)
37. Tan YS, Spring DR, Abell C, Verma CS. 2015 The application of ligand-mapping molecular dynamics simulations to the rational design of peptidic modulators of protein–protein interactions. *J. Chem. Theory Comput.* **11**, 3199–3210. (doi:10.1021/ct5010577)
38. Tan YS *et al.* 2016 Benzene probes in molecular dynamics simulations reveal novel binding sites for ligand design. *J. Phys. Chem. Lett.* **7**, 3452–3457. (doi:10.1021/acs.jpcl.6b01525)
39. Sefah K *et al.* 2014 *In vitro* selection with artificial expanded genetic information systems. *Proc. Natl Acad. Sci. USA* **111**, 1449–1454. (doi:10.1073/pnas.1311778111)
40. Zumrut H, Yang Z, Williams N, Arizala J, Batool S, Benner SA, Mallikaratchy P. 2020 Ligand-guided selection with artificially expanded genetic information systems against TCR-CD3e. *Biochemistry* **59**, 552–562. (doi:10.1021/acs.biochem.9b00919)
41. Zhang L *et al.* 2016 Aptamers against cells overexpressing glypican 3 from expanded genetic systems combined with cell engineering and laboratory evolution. *Angew. Chem. Int. Edn Engl.* **55**, 12372–12375. (doi:10.1002/anie.201605058)
42. Convery MA, Rowsell S, Stonehouse NJ, Ellington AD, Hirao I, Murray JB, Peabody DS, Phillips SE, Stockley PG. 1998 Crystal structure of an RNA aptamer–protein complex at 2.8 Å resolution. *Nat. Struct. Biol.* **5**, 133–139. (doi:10.1038/nsb0298-133)
43. Kimoto M, Tan HP, Tan YS, Mislan NABM, Hirao I. 2023 Success probability of high-affinity DNA aptamer generation by genetic alphabet expansion. Figshare. (doi:10.6084/m9.figshare.c.6328848)